



Research Paper

Melatonin improves cardiac function in a mouse model of heart failure with preserved ejection fraction



Yuan Liu^{a,1}, Li-Na Li^{b,1}, Sen Guo^a, Xiao-Yan Zhao^a, Yu-Zhou Liu^a, Cui Liang^a, Sheng Tu^a, Dan Wang^a, Ling Li^a, Jian-Zeng Dong^a, Lu Gao^{a,*}, Hai-Bo Yang^{a,*}

^a Department of Cardiology, The First Affiliated Hospital of Zhengzhou University, Zhengzhou, China

^b Department of Anaesthesiology, The First Affiliated Hospital of Zhengzhou University, Zhengzhou, China

ARTICLE INFO

Keywords:

Melatonin
HFpEF
CTRP3
Adipocyte
Oxidative stress
Apoptosis

ABSTRACT

Melatonin has been shown to inhibit myocardial infarction-induced apoptosis, its function in heart failure with preserved ejection fraction (HFpEF) has not been investigated. This study aimed to investigate whether melatonin attenuates obesity-related HFpEF. Male mice were fed a high-fat diet (HFD) from weaning to 6 months of age to induce HFpEF. The mice were orally administered melatonin (50 mg/kg) by 3 weeks. Diastolic function was significantly improved by melatonin supplementation in mice fed an HFD. Melatonin attenuated obesity-induced myocardial oxidative stress and apoptosis and promoted the secretion of C1q/tumour necrosis factor-related protein 3 (CTRP3) by adipose tissue. And depletion of circulating CTRP3 largely abolished melatonin-mediated cardio-protection. Melatonin-mediated secretion of adipocyte-derived CTRP3 activated NF-E2-related factor 2 (Nrf2), which were largely abrogated by knocking down CTRP3 in adipocytes or Nrf2 in cardiomyocytes. Nrf2 activation was mediated by miR-200a, and a miR-200a antagomir offset the effects of melatonin-conditioned medium on Nrf2 expression. Our results indicate that melatonin can be used to treat and prevent obesity-related HFpEF.

1. Introduction

Epidemiological studies have reported that heart failure with preserved ejection fraction (HFpEF) accounts for approximately half of all heart failure (HF) cases [1]. More importantly, there is no standard therapy for HFpEF [2]. Therefore, it is greatly important that researchers find a drug that prevents HFpEF development. Obesity is an independent risk factor for HFpEF [3]. Obesity-induced cardiac dysfunction is coordinated by an orchestrated network responsible for inducing numerous pathological phenomena, including oxidative stress and cell apoptosis [4,5]. Theoretically, finding molecules that suppress obesity-induced oxidative stress and cell apoptosis would be of great benefit with respect to the management of HFpEF.

Adipose is now recognised as an endocrine organ. Adipose tissue could secrete a number of adipokines and inflammatory factors, acting on many other metabolically active tissues [6]. Adipose tissue is involved in the pathogenesis of pathological cardiac hypertrophy, systolic dysfunction and HFpEF [6,7], which suggests that functional crosstalk occurs between adipose tissue and the heart. C1q/tumour necrosis factor-related protein 3 (CTRP3), a newly identified factor secreted by

adipocytes [8], plays a key role in cardiometabolic diseases [9]. CTRP3 deficiency in cardiomyocytes increased oxidative stress and cell apoptosis and that CTRP3 overexpression prevented diabetic cardiomyopathy [10]. However, the pathophysiological role of CTRP3 in HFpEF is unknown.

Melatonin is a hormone produced at night by the pineal gland. Melatonin is also a free-radical scavenger and a potent antioxidant [11–13]. Although melatonin has been shown to protect against myocardial infarction-induced apoptosis [14], its function in HFpEF has not been investigated. Previous studies reported that melatonin treatment attenuated obesity in rodents [15,16], and a recent study showed that melatonin induced adipogenesis in adipocytes and alleviated pyroptosis in mouse adipose tissue [17,18]. Given the close interplay between adipose tissue and the heart, we postulated that melatonin causes adipocyte tissue to secrete CTRP3, which improves high-fat diet (HFD)-induced HFpEF. As expected, we found that increases in the secretion of CTRP3 by adipose tissue after melatonin treatment resulted in the specific activation of miR-200a-NF-E2-related factor 2 (Nrf2) in cardiomyocytes to prevent the development of HFpEF.

* Corresponding authors.

E-mail addresses: gaomei1215@163.com (L. Gao), yhb160320@163.com (H.-B. Yang).

¹ These authors contributed equally to this work.

2. Materials and methods

2.1. Reagents

Melatonin and palmitic acid (PA) were purchased from Sigma-Aldrich (St. Louis, MO, USA). Recombinant human CTRP3 (rhCTRP3) was purchased from Aviscera Bioscience (Santa Clara, CA, USA). Anti-B-cell lymphoma-2 (Bcl-2, 1:1000) was obtained from Cell Signaling Technology (Danvers, Massachusetts). Anti-Nrf2 (1:1000), anti-heme oxygenase-1 (HO-1, 1:1000), anti-superoxide dismutase 2 (SOD2, 1:1000), anti-tumour necrosis factor- α (TNF- α , 1:200 for staining), anti-CD68 (1:200 for staining) and anti-CTRP3 (1:500 for western blotting, 1:200 for staining) were purchased from Abcam (Cambridge, UK). Anti-adiponectin (1:200 for staining) was purchased from Proteintech (Chicago, IL, USA). The secondary antibody used in the study was purchased from LI-COR Biosciences (1:10,000 dilution). Dihydroethidium (DHE) was purchased from Invitrogen (Carlsbad, CA, USA). 2',7'-dichlorodihydrofluorescein diacetate (DCFH-DA), total SOD assay kit, catalase (CAT) assay kit, and glutathione (GSH) assay kit were purchased from the Nanjing Jiancheng Bioengineering Institute (Nanjing, China). The mini-osmotic pump was purchased from Alzet (DURECT Corp, Cupertino, CA). Cell counting kit-8 (CCK-8) was obtained from Dōjindo Laboratories (Kumamoto, Japan). All other chemicals were of analytical grade.

2.2. Animals and treatments

All animal experiments were performed according to the guidelines for the Care and Use of Laboratory Animals, which was published by the United States National Institutes of Health (NIH Publication, revised 2011), and were approved by the Animal Care and Use Committee of Zhengzhou University. Male C57/B6 mice (weaning age; body weight: 10–12 g) were purchased from the Institute of Laboratory Animal Science, Chinese Academy of Medical Sciences (Beijing, China). All the mice were housed at a controlled temperature (20–25 °C) and humidity (50 ± 5%) under a 12-h light-dark cycle (light from 6:00 a.m. to 6:00 p.m.) and were allowed free access to food and water. All the mice were fed an HFD (45% kilocalories from fat) or a normal diet (ND, 10% kilocalories from fat) from weaning to 6 months of age. To explore the protective effects of melatonin, 3 weeks before the end of the study, we orally administered the mice melatonin (50 mg/kg) by gavage once daily. The melatonin treatment continued for 3 weeks. One day before the end of the study, we measured the fasting blood glucose levels of the mice. At the end of treatment, all the mice were anaesthetized with isoflurane (1.5%) and subjected to echocardiographic and haemodynamic analyses. All the mice were subsequently euthanized with an overdose of sodium pentobarbital (200 mg/kg; i.p.), and the hearts were dissected to calculate the heart weight (HW)-to-tibia length (TL) ratio. Wet lung weight (LW) and dry LW were also determined. The left ventricles of the hearts were stored at – 80 °C for further study. The mesenteric white adipose tissue (Mes WAT) and subcutaneous white adipose tissue (SC WAT) were also weighed.

2.3. Mini-osmotic pump implantation

To verify that the protective effects of melatonin are mediated by adipose-derived CTRP3, we depleted circulatory CTRP3 using a mini-osmotic pump carrying a CTRP3 antibody. Briefly, all the mice were subcutaneously infused with CTRP3 antibodies (2.5 µg/g/day) or the same volume of IgG by an Alzet osmotic minipump for 4 weeks beginning 1 week before melatonin treatment. To ensure sustained antibody release, we rubbed daily the location at which the minipump was implanted. At the end of the study, we evaluated cardiac diastolic function.

2.4. Echocardiography and pressure-volume analysis

Transthoracic echocardiography was performed as described in the previous studies [10,19–23]. Briefly, the left hemithorax of each mouse was shaved under isoflurane (1.5%) anaesthesia, and echocardiography was performed by a MyLab 30CV ultrasound machine (Esaote SpA, Genoa, Italy) with a 10-MHz linear array ultrasound transducer. M-mode images of the left ventricle were recorded at the level of the papillary muscle. Heart rate and the systolic intraventricular septum (IVSs), left ventricle (LV) end-diastolic dimension (LVIDd) and ejection fraction (EF) were measured. All measurements represent the average of five cardiac cycles and were performed by the same observer.

Pressure-volume analysis was performed as described previously [10,19–23]. The mouse carotid artery was isolated, and a 1.4 French Millar catheter transducer (SPR-839; Millar Instruments, Houston, TX, USA) was advanced from the right carotid artery into the LV under deep anaesthesia. The data were then analysed by PVAN data analysis software.

2.5. Histological analysis

The hearts were fixed with 4% formaldehyde overnight. After dehydration, the hearts were embedded in paraffin and cut into sections. To observe morphometric alterations, we stained the sections with haematoxylin and eosin (H&E) to outline the cross-sectional area of the cardiomyocytes and picrosirius red (PSR) to evaluate cardiac fibrosis, as described in the previous studies [10,19–23]. The cross-sectional area and fibrotic area were measured with a digital analysis system (Image-Pro Plus 6.0, Media Cybernetics, Bethesda, MD, USA) using light-microscopic images of the heart sections. To outline the cardiomyocyte area, we analysed a total of 200 cells in 5 mice. Adipose tissues were also fixed in 4% formaldehyde overnight and embedded in paraffin. These sections were then stained with H&E. The diameter of the adipocytes (Mes WAT) was measured using Image-Pro Plus 6.0. A total of 200 cells in 5 mice were analysed. All the sections were examined by two authors without knowledge of the treatments to which the tissues had been subjected.

2.6. Quantitative real-time PCR and western blotting

Total RNA was prepared using TRIzol reagent (Invitrogen) from heart samples and Mes WAT. Two micrograms of RNA was reverse-transcribed into cDNA with random primers using a Transcriptor First Strand cDNA Synthesis Kit [Roche (Basel, Switzerland), 04896866001]. Real-time PCR was performed using LightCycler 480 SYBR Green 1 Master Mix (Roche, 04707516001). The PCR reaction conditions were as follows: 95 °C for 10 min, followed by 40 cycles of 5 °C for 10 s, 60 °C for 10 s and 72 °C for 20 s and a final step at 72 °C for 10 min. *Gapdh* was used as an internal reference. All the primers used for the experiment are provided in Table S1. miRNA levels were detected using a Bulge-Loop™ miRNA qRT-PCR System, which was obtained from Guangzhou RiboBio Co., Ltd. (Guangzhou, China). *U6* was used as a miRNA internal reference.

Western blotting was performed as previously described [20]. Frozen heart samples and cells were harvested in RIPA lysis buffer, and then the proteins were separated on 10% SDS-PAGE and transferred onto PVDF membranes (Merck Millipore), which were blocked with nonfat milk for 1 h at room temperature before probed with antibodies to CTRP3 (1:500), Nrf2 (1:1000), HO-1 (1:1000), SOD-2 (1:1000) and GAPDH (1:1000) for 12 h at 4 °C. The membranes were then incubated with the appropriate secondary antibody for 1 h at room temperature. The membranes were scanned, and the relative expression levels of the proteins were normalized to that of GAPDH.

2.7. CTRP3 detection

Circulating CTRP3 levels were determined by commercial ELISA kit (Aviva Systems Biology, San Diego, CA) according to manufacturer's instructions.

2.8. Biochemical analysis and 4-hydroxynonenal detection

Fresh heart samples were homogenized on ice and centrifuged at 3000 rpm for 15 min. After that, and the supernatants were collected to measure the activities of SOD and CAT as well as the content of GSH by commercial kits according to manufacturer's instructions. 4-Hydroxynonenal (4-HNE) in the heart tissues were determined using the kit obtained from Cell Biolabs (San Diego, USA).

2.9. Cell culture

H9c2 cells and 3T3-L1 preadipocytes were purchased from the Cell Bank of the Chinese Academy of Sciences (Shanghai, China). The purity of the cell lines was confirmed with short tandem-repeat DNA profiling. No mycoplasma contamination was noted in our study. Cells below passage 15 were used in our experiments. The H9c2 cells were cultured in Dulbecco's modified Eagle medium (DMEM, GIBCO, C11995) supplemented with 10% foetal bovine serum (FBS, GIBCO, 10099) and 1% penicillin-streptomycin at 37 °C in a humidified atmosphere with 5% CO₂. The cells were seeded in 6-well plates in DMEM with 10% FBS for 48 h. To investigate the effect of melatonin on CTRP3 levels in cardiomyocytes, we starved the cells for 16 h and then treated them with melatonin (10 μmol/L), which was dissolved in 0.1% DMSO. The 3T3-L1 cells were initially also cultured in DMEM/F12 containing 10% FBS. At confluence, the 3T3-L1 preadipocytes were differentiated into adipocytes by treatment with differentiation medium comprising DMEM/F12, 10% FBS, 1.0 μM dexamethasone, 0.5 mM methylisobutylxanthine and 1.0 μg/ml insulin for 4 days. After 4 days, the differentiation medium was replaced by serum-free medium with 1.0 μg/ml insulin, and the adipocytes were treated with melatonin (10 μmol/L) or vehicle for 24 h. The conditioned medium was collected to stimulate the cardiomyocytes after any residual cells were removed by centrifugation. We selected a period of 4 days because a previous study showed that CTRP3 protein expression was induced at a high level after 4 days of adipocyte differentiation [8]. The H9c2 cells were incubated in dialyzed conditioned medium for 24 h and then treated with PA (500 μmol/L) or 0.1% DMSO PBS. To detect Nrf2 translocation, we stimulated the H9c2 cells with PA for 30 min. The H9c2 cells were stimulated with PA for 24 h for RNA extraction and reactive oxygen species (ROS) detection. To detect apoptosis, we stimulated the H9c2 cells with PA for 48 h.

2.10. Adenovirus vector construction and siRNA transfection

Adenoviral vectors carrying CTRP3 small hairpin RNAs (shRNAs) designed to knock down CTRP3 in adipocytes were generated by Hanbio (Shanghai, China). Scrambled shRNA was used as a control. Briefly, adipocytes were incubated in DMEM/F12 and were infected with adenoviral vectors at a multiplicity of infection (MOI) of 100 for 4 h. To knock down Nrf2 in H9c2 cells, we purchased siNrf2 and negative-control siRNA from Guangzhou RiboBio Co., Ltd. H9c2 cells were transfected with siNrf2 using Lipofectamine RNAiMAX (Invitrogen) for 24 h. Transfection efficiency was confirmed by western blotting. AntagomiR-200a and a miRNA inhibitor control, which were obtained from Guangzhou RiboBio Co., Ltd, were used to silence miR-200a in H9c2 cells.

2.11. DHE staining, TUNEL staining and immunostaining

Cryosections of fresh heart samples were stained with DHE (10 μM)

for 30 min at 37 °C to detect ROS production. Pictures were taken with an OLYMPUS DX51 fluorescence microscope (Tokyo, Japan). HFD-related cardiac injury was detected using TUNEL staining, according to the manufacturer's instructions (S7165, Millipore). Immunofluorescence analysis of the heart sections was performed using cryosections, which were incubated with α-actin antibody (1:200) and CTRP3 antibody (1:200) overnight at 4 °C before being incubated with Alexa568-conjugated goat-anti mouse (1:200) and Alexa488-conjugated goat-anti mouse (1:200). After being stained with DAPI, these sections were observed under an OLYMPUS DX51 fluorescence microscope (Tokyo, Japan). Immunofluorescence analysis of the Mes WAT samples was performed using paraffin-embedded sections. Briefly, after antigen retrieval, the paraffin-embedded sections (5 μm) were incubated with CTRP3 antibody (1:200) and adiponectin antibody (1:200) overnight at 4 °C before being incubated with Alexa568-conjugated goat-anti mouse (1:200) for 30 min at 37 °C. After being mounted and observed by fluorescence microscopy, all the sections were examined by two authors without knowledge of the treatments to which the samples had been subjected. To evaluate Nrf2 nuclear translocation, we fixed H9c2 cells with 4% formaldehyde and permeabilized them in 0.5% Triton X-100, after which we stained them with anti-Nrf2 (dilution: 1:100) in 1% donkey serum overnight at 4 °C before incubating them with Alexa Fluor 568-goat anti-mouse for 30 min at 37 °C. We then stained them with DAPI. The slides were examined in a blinded manner under an OLYMPUS DX51 fluorescence microscope.

2.12. DCFH-DA staining and cell viability assay

To detect ROS production in vitro, we incubated H9c2 cells with DCFH-DA in the dark for 30 min at 37 °C. After being washed 3 times with PBS, the H9c2 cells were visualized in a blinded manner under an Olympus IX53 fluorescence microscope. Cell viability was determined by CCK-8 assay (Dojindo Molecular Technologies, Rockville, MD, USA), according to the manufacturer's protocol and as described previously [10].

2.13. Statistical analysis

The sample size in each group is indicated in the figure legends. Each independent in vitro experiment was performed in triplicate. The data are expressed as the mean ± standard deviation (SD), and all the data were analysed using SPSS 19.0 software. One-way ANOVA followed by Tukey's post hoc test was performed for comparisons among more than two groups. Differences between two groups were assessed using an unpaired, two-sided Student's *t*-test.

3. Results

3.1. Melatonin attenuated body weight gain and the HFpEF phenotype caused by HFD administration in mice

To investigate the effect of melatonin on body weight gain after HFD administration, we administered melatonin (50 mg/kg) orally to mice at 3 weeks beginning at 18 weeks after HFD. We determined this time point for the reason that diastolic function began to decrease at 18 weeks after HFD according to our preliminary data (Fig. S1A). Melatonin treatment beginning at 18 weeks after HFD allowed us to investigate whether melatonin would attenuate advanced (pre-existed) cardiac remodelling induced by obesity, which is of clinical significance. Daily melatonin treatment for 3 weeks attenuated body weight, whole animal weight gain, hyperglycaemia and Mes WAT deposition in HFD-fed mice without affecting SC WAT deposition (Fig. S1B, Fig. 1A–D). Mes WAT was collected for H&E staining and cell area was also determined. The results of our study demonstrated that cell areas were smaller in mice treated with HFD + melatonin than in mice

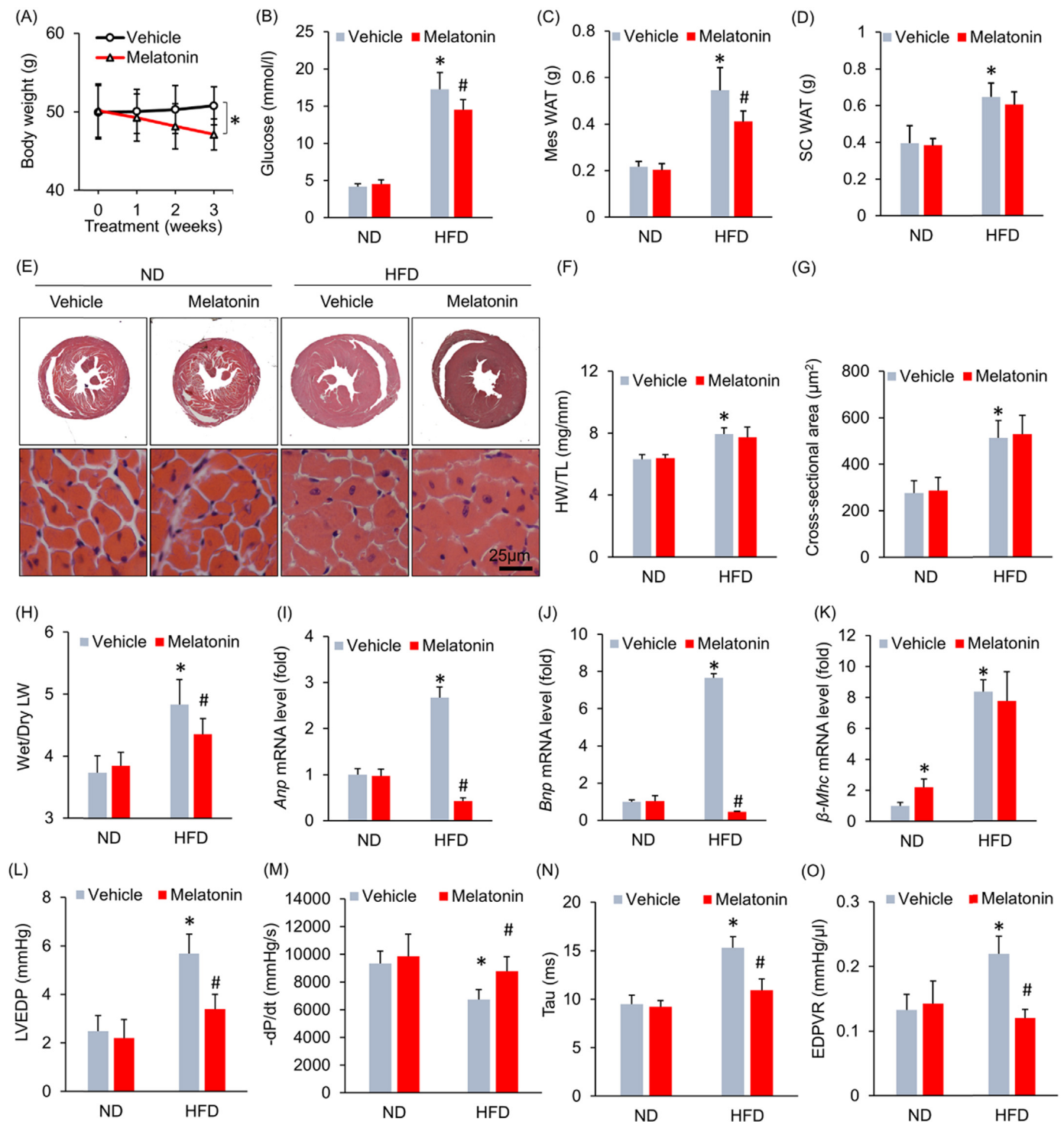


Fig. 1. Melatonin treatment attenuated obesity-related heart failure with preserved ejection fraction without affecting the cardiac hypertrophy phenotype. (A) Alterations in body weight after melatonin treatment for 3 weeks (n = 9 per group). (B) Blood glucose levels with melatonin treatment (n = 9 per group). (C–D) Alterations in Mes WAT and SC WAT after melatonin treatment (n = 9 per group). (E) Representative images of HE-stained heart sections. (F) Results for the of the HW/TL ratio (n = 9 per group). (G) The left ventricular cross-sectional area in the indicated groups (n = 5 per group). (H) The wet LW-to-dry LW ratio (n = 9 per group). (I–K) *Anp*, *Bnp* and β -*Mhc* mRNA levels after melatonin treatment (n = 6 per group). (L) LVEDP after melatonin treatment (n = 9 per group). (M) -dP/dt with melatonin treatment (n = 9 per group). (N) Alteration in the Tau index after melatonin treatment (n = 9 per group). (O) Alteration in the EDPVR (n = 9 per group). All data are expressed as the mean \pm SD. For (A), one-way repeated measure analysis of variance (ANOVA) was used, **P* < 0.05. For (B–O), differences were compared by one-way ANOVA followed by Tukey’s post hoc test. **P* < 0.05 compared with the ND + vehicle group, #*P* < 0.05 compared with the HFD + vehicle group.

treated with HFD + vehicle (Fig. S1C). We next examined the effect of melatonin on cardiac structure and function. Unexpectedly, long-term HFD administration caused equivalent hypertrophy in mice

supplemented with or without melatonin, as evidenced by the histological staining results, the HW-to-TL ratio data and the cell cross-sectional area measurements (Fig. 1E–G). HFD administration significantly

increased the wet LW to dry LW ratio, changes reflecting lung congestion, in mice that did not receive melatonin treatment. However, the wet LW to dry LW ratio in HFD-fed mice that were treated with melatonin were significantly lower than those in HFD-fed mice that did not receive melatonin treatment (Fig. 1H). Subsequent analysis of the mRNA expression levels of several genes indicated that melatonin decreased HFD-induced *Anp* and *Bnp* mRNA expression (Fig. 1I–J). Melatonin increased β -*Mhc* mRNA levels in mice fed an ND but had no effect on β -*Mhc* mRNA levels in mice fed an HFD (Fig. 1K). To corroborate our hypothesis that melatonin prevents HFD-induced HFpEF, we performed echocardiography and pressure-volume analysis. As shown in Fig. S2A–C, there were no differences in heart rate, LVIDd and IVSs between the vehicle- and melatonin-treated groups, regardless of whether the groups received an ND or HFD. Moreover, there was no difference in cardiac systolic function, as indicated by the EF, LV end-systolic pressure (LVESP) and +dP/dt results, among all the groups (Fig. S2D–F). Pressure-volume analysis showed that diastolic dysfunction was attenuated in melatonin-treated obese mice compared with vehicle-treated obese mice, an effect that presented as a decrease in LV end-diastolic pressure (LVEDP) in the former group (Fig. 1L). Impairments in active relaxation were also prevented in melatonin-treated obese mice, as these mice displayed an increased -dP/dt (Fig. 1M) and a decreased Tau index compared with vehicle-treated obese mice (Fig. 1N). The end-diastolic pressure-volume relationship (EDPVR), which is an index of passive cardiac stiffness, decreased to almost its normal level after 3 weeks of melatonin treatment (Fig. 1O).

3.2. Melatonin decreased cardiac oxidative injury and cardiomyocyte apoptosis in mice with HFpEF

Cardiac fibrosis is an important cause of left ventricular stiffening [24]. Therefore, we determined whether melatonin attenuated HFD-induced cardiac fibrosis. HFD administration resulted in an increase in collagen volume, a pathologic change that was not attenuated after melatonin treatment (Fig. S3A–B). This finding was confirmed by a subsequent fibrotic marker analysis, which showed that melatonin slightly inhibited *collagen I* expression without affecting *collagen III* expression (Fig. S3C–D). Melatonin is a potent antioxidant [11] and ROS are involved in the pathogenesis of HFpEF [25]. Thus, we subsequently detected ROS production in the heart using DHE staining. HFD administration resulted in excessive ROS production, and melatonin supplementation almost completely inhibited ROS production (Fig. 2A–B). HFD administration led to decreases in *Sod2* and *Gpx* mRNA levels, pathological alterations that were reversed by melatonin supplementation (Fig. 2C–D). Further detection revealed that the decreased activities of SOD and CAT were restored by melatonin treatment (Fig. 2E–F). HFD treatment led to a decrease in GSH level, an increase in the level of 4-HNE. These pathological alterations were reversed after melatonin treatment (Fig. 2G–H). Western blot analysis indicated that HFD-induced decreases in Nrf2, SOD2 and HO-1 expression were reversed by melatonin supplementation (Fig. 2I). Excessive ROS production resulted in cardiomyocyte apoptosis. TUNEL staining indicated that melatonin inhibited HFD-induced cell loss in the heart (Fig. 2J–K). This finding was supported by the western blot analysis results, which showed that melatonin upregulated the expression of Bcl-2, which is an anti-apoptotic factor (Fig. 2L).

3.3. Melatonin exerted cardio-protection by causing adipocytes to secrete CTRP3

A previous study demonstrated that CTRP3 inhibited oxidative stress and cell apoptosis in diabetic hearts [10]; therefore, we next detected the effect of melatonin on myocardial CTRP3 expression. As shown in Fig. 3A–C, melatonin significantly increased myocardial CTRP3 expression after HFD administration but did not alter myocardial CTRP3 expression under basal conditions (Fig. 3A–C). The

previous study reported that CTRP3 was also expressed in cardiomyocytes and that CTRP3 deficiency in cardiomyocytes increased oxidative stress levels and cell apoptosis [10]. Thus, we subsequently identified the cell type that contributed to the increase in CTRP3 expression in the heart after melatonin treatment. H9c2 cardiomyocytes were treated with melatonin. As shown in Fig. 3D–E, CTRP3 expression levels in H9c2 cells treated with escalating doses of melatonin were not statistically distinguishable from those in controls treated with only 0.1% DMSO. An initial study found that CTRP3 was expressed in and secreted predominantly by adipose tissue [26]. To verify this and to exclude other sources of CTRP3, we detected the mRNA expression of CTRP3 in other organs. We found that CTRP3 mRNA in the adipose tissue was about approximately 36 times higher than that in heart and 182 times higher than that in liver (Fig. S4A). Next, we detected the alteration of CTRP3 during HFD, and found adipose tissue was the only organ with significant alteration in CTRP3 mRNA level (Fig. S4B). Thus, we used 3T3-L1 adipocytes in subsequent experiments. Interestingly, melatonin (10 μ mol/L) significantly induced CTRP3 production in a time-dependent manner in adipocytes (Fig. 4A). To support this finding, we collected Mes WAT and performed immunofluorescence to detect CTRP3 expression in adipose tissue and found that melatonin increased CTRP3 expression in the adipose tissue of obese mice (Fig. 4B–C). Next, we detected circulating CTRP3 level and found that circulating CTRP3 expression decreased significantly after HFD administration (ND + vehicle: 572.04 \pm 11.25 ng/ml; HFD + vehicle: 288.97 \pm 20.98 ng/ml) and was restored to almost its normal level (HFD + melatonin: 502.27 \pm 12.93 ng/ml) after melatonin supplementation for 3 weeks (Fig. 4D). Adipose tissue is an endocrine organ and secretes adiponectin and inflammatory factors, which may act on the heart. To exclude the possibility that adiponectin was involved in melatonin-mediated protection, we detected adiponectin expression in adipose tissue. We noted no difference in adiponectin expression between the HFD + vehicle and HFD + melatonin groups (Fig. 4E). Detection of the mRNA levels of various genes indicated that melatonin treatment could not attenuate HFD-induced increases in *Tnf- α* , *Il-6* and *Mcp-1* mRNA levels in adipose tissue (Fig. S4C). To determine the contribution of CTRP3, which is secreted by adipose tissue, to cardiac function, we blocked circulating CTRP3 activity using an ALZET osmotic pump that delivered CTRP3 antibodies for 4 weeks. As expected, one week after CTRP3 antibody infusion (the time point of melatonin treatment), the circulating CTRP3 was almost depleted (Fig. S4D). The circulating CTRP3 concentration in mice that received a 4-week infusion of CTRP3 antibodies decreased to a level that was 22.5% of that in mice that received an infusion of IgG (IgG infusion: 566.54 \pm 20.09 ng/ml; CTRP3 antibody infusion: 127.27 \pm 15.95 ng/ml, Fig. S5A). Moreover, blocking circulating CTRP3 expression in mice treated with HFD + melatonin resulted in aggravated cardiac diastolic function, which presented as alterations in LVEDP, dP/dtmin and the Tau index (Fig. 5A–C). We noted no difference in LVEDP, dP/dtmin and the Tau index between the HFD + vehicle + anti-CTRP3 and HFD + melatonin + anti-CTRP3 groups (Fig. 5A–C). Blocking circulating CTRP3 also completely abolished the inhibitory effects of melatonin on oxidative stress induced by HFD, as reflected by the alteration in 4-HNE content, the mRNA levels of *Sod2* and *Gpx* (Fig. 5D–F).

3.4. Melatonin activated cardiac Nrf2 via CTRP3 secreted by adipocytes

The medium in which 3T3-L1 adipocytes had been incubated was collected and pooled, and then CTRP3 levels in the conditioned medium were detected. As expected, CTRP3 levels were increased in the conditioned medium after melatonin treatment (Fig. 6A). H9c2 cardiomyocytes were then incubated with the medium in which melatonin- or vehicle-treated adipocytes had been incubated. Similar to rhCTR3, the conditioned medium in which melatonin-treated adipocytes had been incubated increased Nrf2, HO-1 and SOD2 expression in H9c2 cells in a time-dependent manner (Fig. 6B–C). Moreover, the conditioned

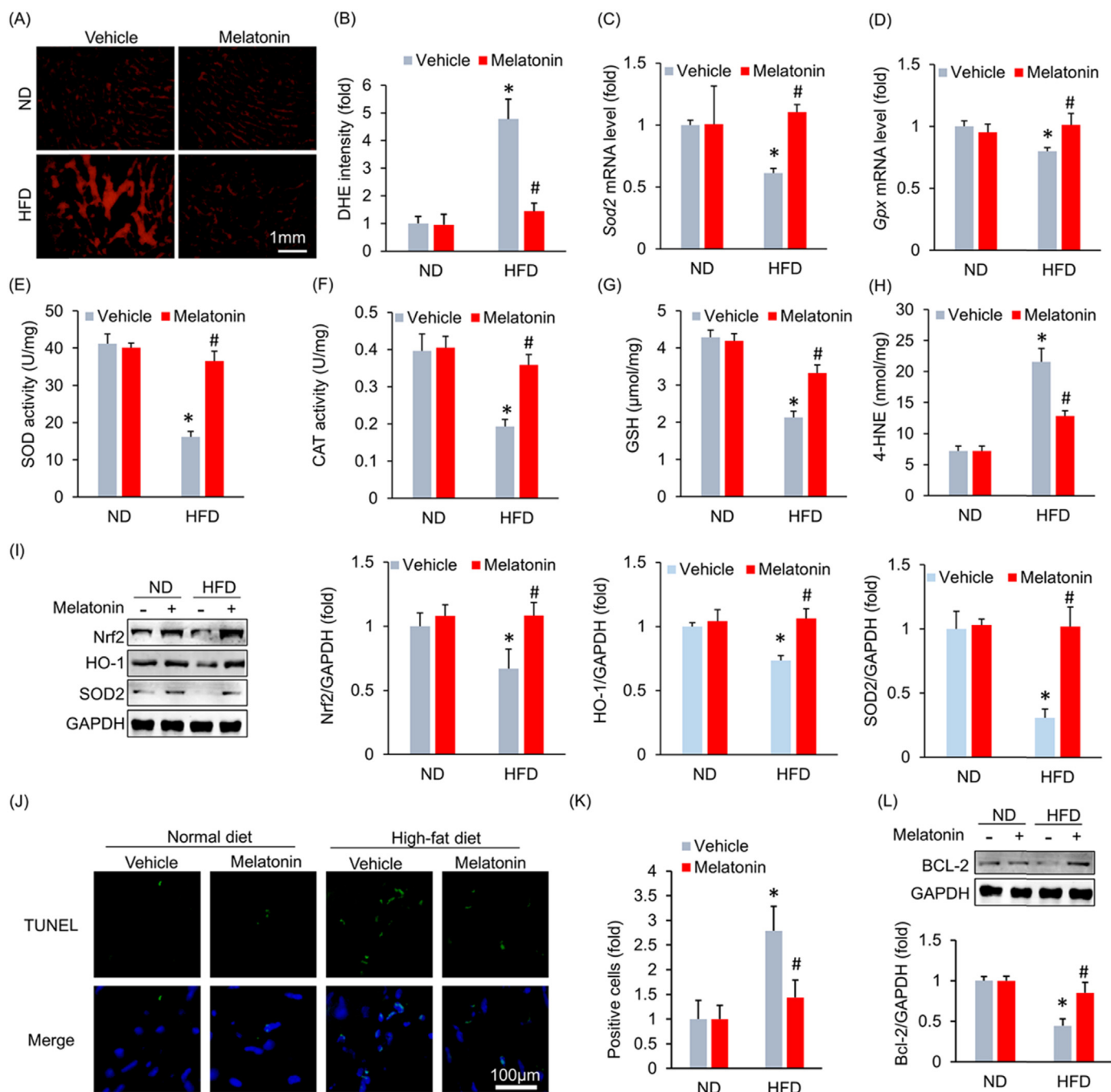


Fig. 2. Melatonin attenuated obesity-induced myocardial oxidative stress and myocardial apoptosis. (A–B) Representative images and results for DHE staining ($n = 5$ per group). (C–D) *Sod2* and *Gpx* mRNA levels after melatonin treatment ($n = 6$ per group). (E–F) The activities of SOD and CAT after melatonin treatment ($n = 6$ per group). (G) The content of GSH ($n = 6$ per group). (H) The level of 4-HNE ($n = 6$ per group). (I) Representative blots and results for Nrf2, HO-1 and SOD2 ($n = 6$ per group). (J–K) Representative images and results of TUNEL staining ($n = 5$ per group). (L) Bcl-2 protein expression levels after melatonin treatment ($n = 6$ per group). All data are expressed as the mean \pm SD. Differences were compared by one-way ANOVA followed by Tukey's post hoc test. * $P < 0.05$ compared with the ND + vehicle group, # $P < 0.05$ compared with the HFD + vehicle group.

medium in which melatonin-treated adipocytes had been incubated promoted Nrf2 translocation into the nucleus (Fig. 6D). PA stimulation led to a decrease in Nrf2 accumulation in H9c2 cell nuclei, a pathological change that was reversed after the cells were incubated in the medium in which melatonin-treated adipocytes had been incubated (Fig. 6D). CTRP3 deficiency in adipocytes almost completely abolished Nrf2 and HO-1 upregulation in H9c2 cells (Fig. S6A, Fig. 6E–F). We subsequently investigated whether Nrf2 activation contributed to the protective effects of the medium in which melatonin-treated adipocytes had been incubated. We knocked down CTRP3 in adipocytes (Fig. S5A)

or Nrf2 in cardiomyocytes (Fig. S6B) and found that CTRP3 deficiency in adipocytes or Nrf2 deficiency in cardiomyocytes blocked the protective effects of the medium in which melatonin-treated adipocytes had been incubated on cell viability (Fig. 6G). The upregulation of *Sod2* expression was also abrogated by CTRP3 deficiency in adipocytes and Nrf2 deficiency in cardiomyocytes (Fig. 6H). DCFH-DA and TUNEL staining showed that the protective effects of the above medium against oxidative stress and cell apoptosis were also abolished by CTRP3 deficiency in adipocytes or Nrf2 deficiency in cardiomyocytes (Fig. 6I).

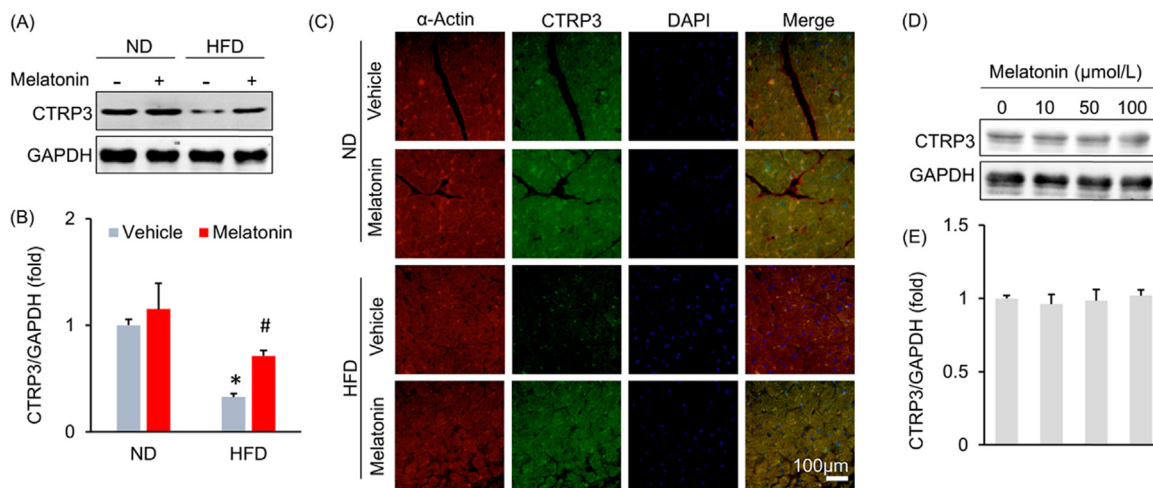


Fig. 3. Melatonin increased myocardial CTRP3 expression in obese mice. (A–B) Representative blots and results for myocardial CTRP3 expression (n = 6 per group). (C) Representative images of myocardial CTRP3 immunostaining. (D–E) CTRP3 expression in H9c2 cells. H9c2 cells were treated with melatonin for 15 min, after which they were collected for blot detection. Data are expressed as the mean ± SD of six independent experiments (D–E). Differences were compared by one-way ANOVA followed by Tukey’s post hoc test. *P < 0.05 compared with the ND+vehicle group, #P < 0.05 compared with the HFD+vehicle group.

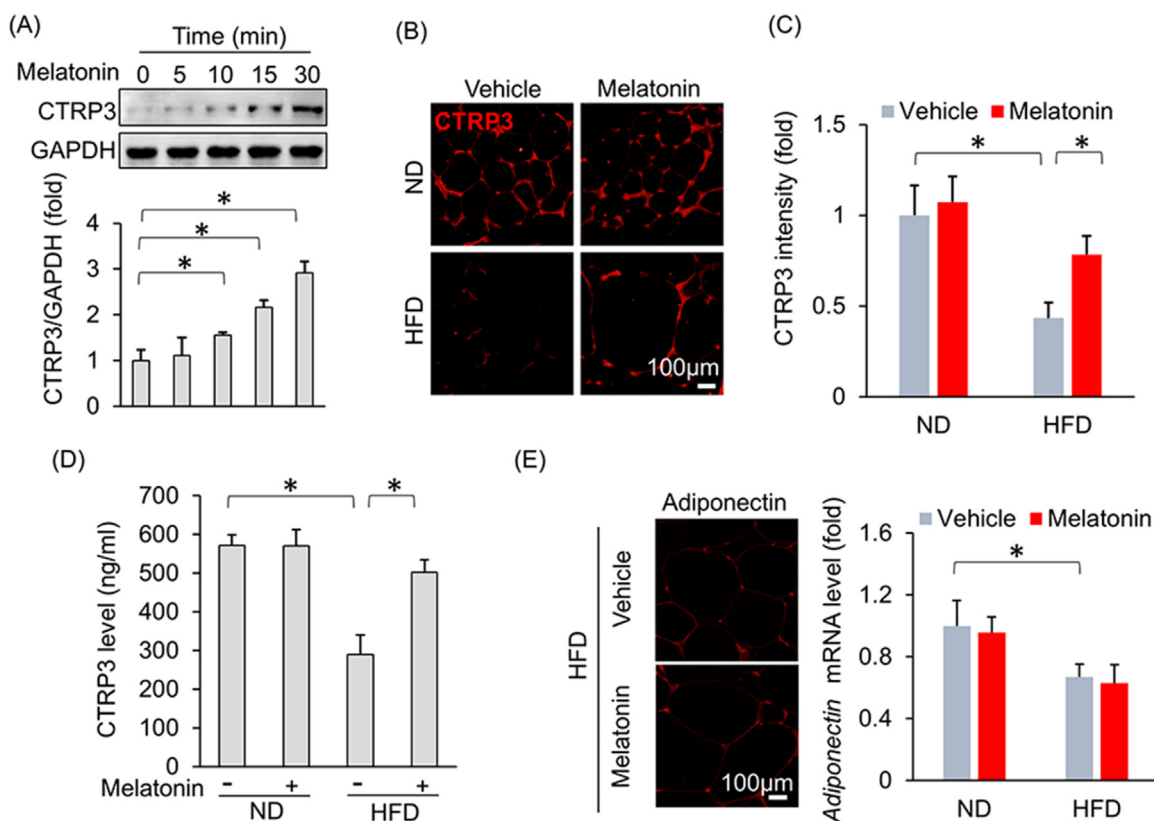


Fig. 4. Melatonin caused adipocytes to secrete CTRP3 without affecting adiponectin expression or inflammation. (A) CTRP3 expression in 3T3-L1 adipocytes. 3T3-L1 adipocytes were subjected to treatment with melatonin (10 μmol/L) at different time points and then collected for blot detection. (B–C) Representative images and results for CTRP3 immunostaining in adipose tissue after melatonin treatment (n = 5 per group). (D) Circulating CTRP3 levels after melatonin treatment (n = 6 per group). (E) The level of adiponectin in adipose tissues (n = 5 per group). Data are expressed as the mean ± SD of six independent experiments (A). Differences were compared by one-way ANOVA followed by Tukey’s post hoc test. *P < 0.05.

3.5. miR-200a was involved in myocardial Nrf2 activation after melatonin treatment

We subsequently determined the effects of miRNA on Nrf2 transcription. All the miRNAs that have been reported to regulate the level of Nrf2 were detected, including miR-144, miR-27a, miR-142a, miR-153, miR-93, miR-28a, miR-365, miR-193b and miR-200a [27]. miR-93

expression decreased, while miR-193b and miR-200a expression increased after cardiomyocytes were incubated in the medium in which melatonin- or vehicle-treated adipocytes had been incubated (Fig. 7A). rhCTR3 supplementation also increased miR-200a levels (Fig. 7B). Previous study reported that miR-200a ameliorates diabetic nephropathy [28]. Therefore, we concluded that miR-200a may be involved in the Nrf2 activation induced by the medium in which adipocytes had

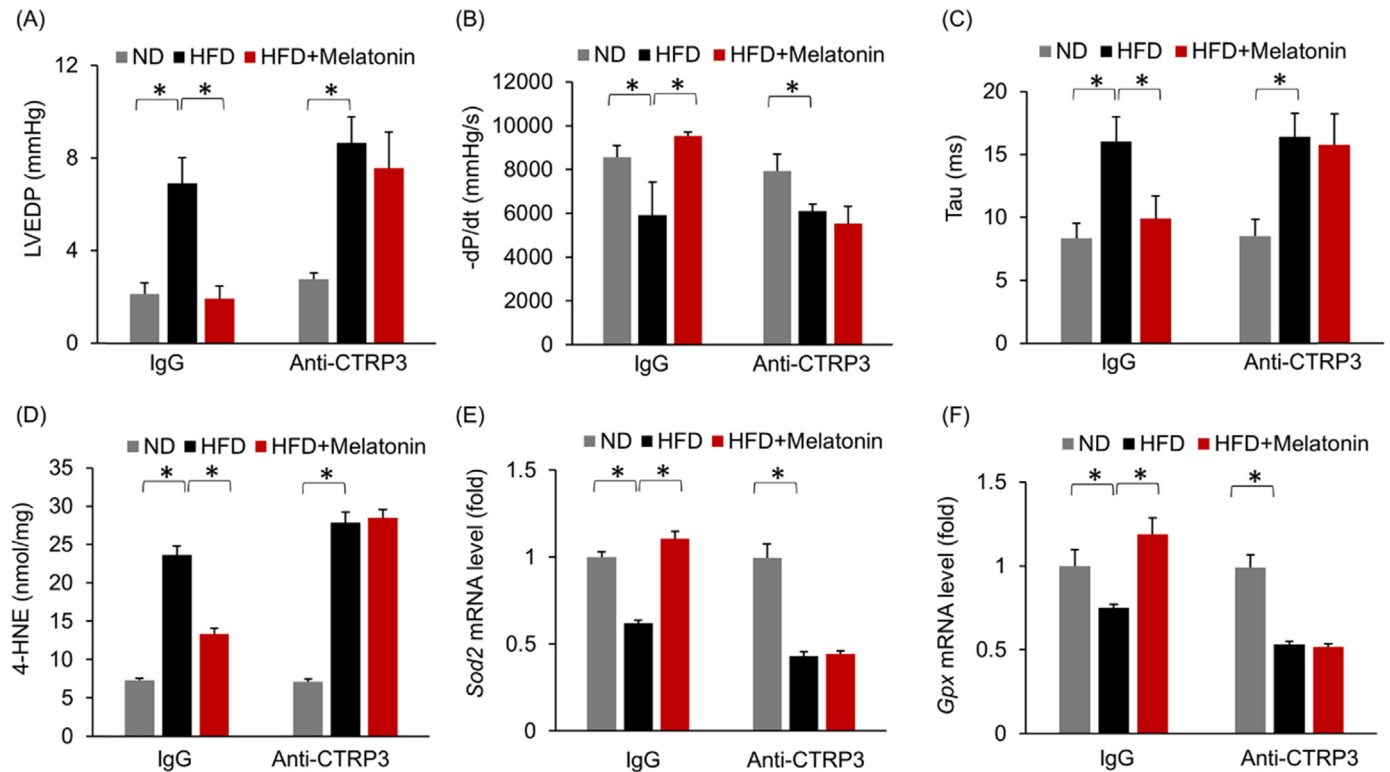


Fig. 5. Depleting circulating CTRP3 using a CTRP3 antibody largely abolished melatonin-mediated protection against diastolic dysfunction. (A) LVEDP after melatonin treatment (n = 5 per group). (B) -dP/dt with melatonin treatment (n = 5 per group). (C) Alterations in the Tau index after melatonin treatment (n = 5 per group). (D) The level of 4-HNE (n = 5 per group). (E-F) The mRNA levels of *Sod2* and *Gpx* (n = 5 per group). All data are expressed as the mean \pm SD. Differences were compared by one-way ANOVA followed by Tukey's post hoc test. * $P < 0.05$.

been incubated. Kelch-like ECH-associating protein 1 (Keap1) interacts with Nrf2 and retains Nrf2 in the cytoplasm [29]. miR-200a targets the 3'-UTR of *Keap1*, leading to destabilization of *Keap1* mRNA and a reduction in Keap1 protein level [30]. Thus, we measured *Keap1* mRNA levels and found that they were decreased in cardiomyocytes that were incubated in the medium in which melatonin-treated adipocytes had been incubated but were upregulated after antagomiR-200a treatment (Fig. S7A, Fig. 7C). Western blot analysis showed that the increases in Nrf2 and HO-1 expression caused by melatonin-conditioned medium were also abolished by antagomiR-200a (Fig. 7D–F). AntagomiR-200a also offset the protective effects of melatonin-conditioned medium against cardiomyocyte apoptosis (Fig. S7B).

4. Discussion

Here, we revealed that melatonin plays a previously unrecognized role in HFpEF. Our results suggested that melatonin has a protective effect against obesity-related HFpEF and improves diastolic function. Melatonin blocked myocardial ROS production and cell apoptosis induced by long-term HFD administration. The cardioprotective effects of melatonin were mediated by adipose tissue-derived CTRP3, which activated Nrf2 via miR-200a. Blocking circulating CTRP3 or knocking down CTRP3 in adipocytes completely abolished the protective effects of melatonin. Medium that was collected from cultures in which melatonin-treated adipocytes had been incubated also failed to protect cardiomyocytes with Nrf2 deficiency or miR-200a inhibition.

Obesity is closely related to HFpEF, a condition with high mortality. The association between HFpEF and metabolic syndrome has not been well-studied. Moreover no specific therapy for HFpEF has been identified. Theoretically, finding drugs that prevent obesity- and metabolic syndrome-related HFpEF would be important for the treatment of the disease. A previous study indicated that melatonin supplementation

reduced body weight gain, a change that was not dependent on a reduction in food intake [31,32]. Furthermore, considerable evidence indicates that melatonin has protective effects in cardiovascular diseases. Melatonin protected against cardiac ischaemia-reperfusion injury [14] and cardiac hypertrophy [33]. These observations suggested that melatonin attenuates obesity-related HFpEF. Our data clearly demonstrated that melatonin ameliorated diastolic dysfunction without effecting cardiac hypertrophy or cardiac fibrosis in HFpEF mice. Our findings support further clinical exploration of a potential therapeutic role for melatonin in obesity-related HFpEF.

There is a consensus that crosstalk occurs between adipose tissues and hearts. Adiponectin, which is secreted by human adipose tissue, protected against myocardial oxidative stress [34]. PPAR- γ deficiency in adipocytes attenuates the hypertrophic response [35]. However, the precise molecular players that mediate this crosstalk remain unknown. Increases in visceral adipose mass lead to the secretion of inflammatory cytokines at higher levels, which results in an increase in systemic inflammation [36]. We sought to verify the hypothesis that the protective effects of melatonin are attributable to alterations in the levels of inflammatory cytokines secreted by adipose tissues. Our results suggested that inflammatory cytokine levels were similar between the HFD + melatonin group and the HFD + vehicle group, implying that the protective effects of melatonin are not attributable to alterations in the levels of inflammatory cytokines secreted by adipose tissues. The circulating level of adiponectin was decreased in obesity [37], and adiponectin overexpression prevented the progression of aldosterone-induced HFpEF [38]. The finding that melatonin could not affect the levels of adiponectin in adipose tissue suggested that melatonin supplementation attenuated HFpEF independent of adiponectin. The results of our study indicated that melatonin treatment resulted in an increase in the release of CTRP3 into the circulatory system and increased cardiac CTRP3 expression in obese mice. Conversely, blocking

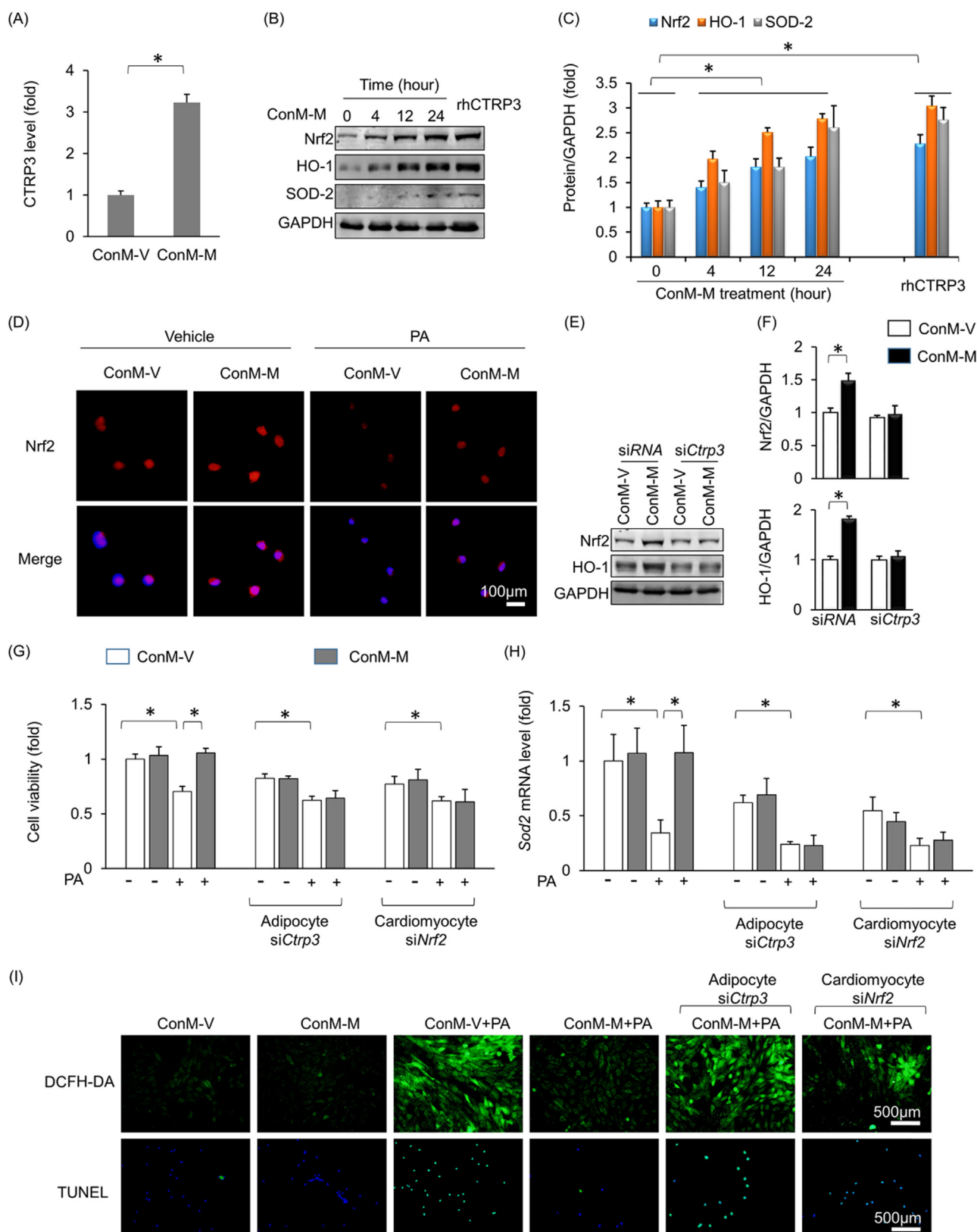


Fig. 6. Adipocyte-derived CTRP3 activated Nrf2 to prevent oxidative stress and cell apoptosis. (A) CTRP3 expression in the pooled adipocyte medium. 3T3-L1 adipocytes were treated melatonin (10 µmol/L) or vehicle for 24 h, after which the medium was collected to detect CTRP3 expression. ConM-V: conditioned medium in which adipocytes treated with vehicle were cultured; ConM-M: conditioned medium in which adipocytes treated with melatonin were cultured. (B-C) Nrf2, HO-1 and SOD2 expression in H9c2 cells. H9c2 cells were exposed to ConM-M for different time periods and then collected for blot detection. (D) Immunostaining of Nrf2 in H9c2 cells. H9c2 cells were exposed to ConM-V or ConM-M for 4 h and then collected for blot detection. (E-F) CTRP3 deficiency in adipocytes largely abolished the effects ConM-M on Nrf2 and HO-1 expression in H9c2 cells. (G) Cell viability in all the groups. (H) *Sod2* mRNA levels in H9c2 cells. (I) DCFH-DA staining and TUNEL staining. rhCTRTP3, recombinant human CTRP3. All data are expressed as the mean ± SD of six independent experiments. Differences were compared by one-way ANOVA followed by Tukey's post hoc test. **P* < 0.05.

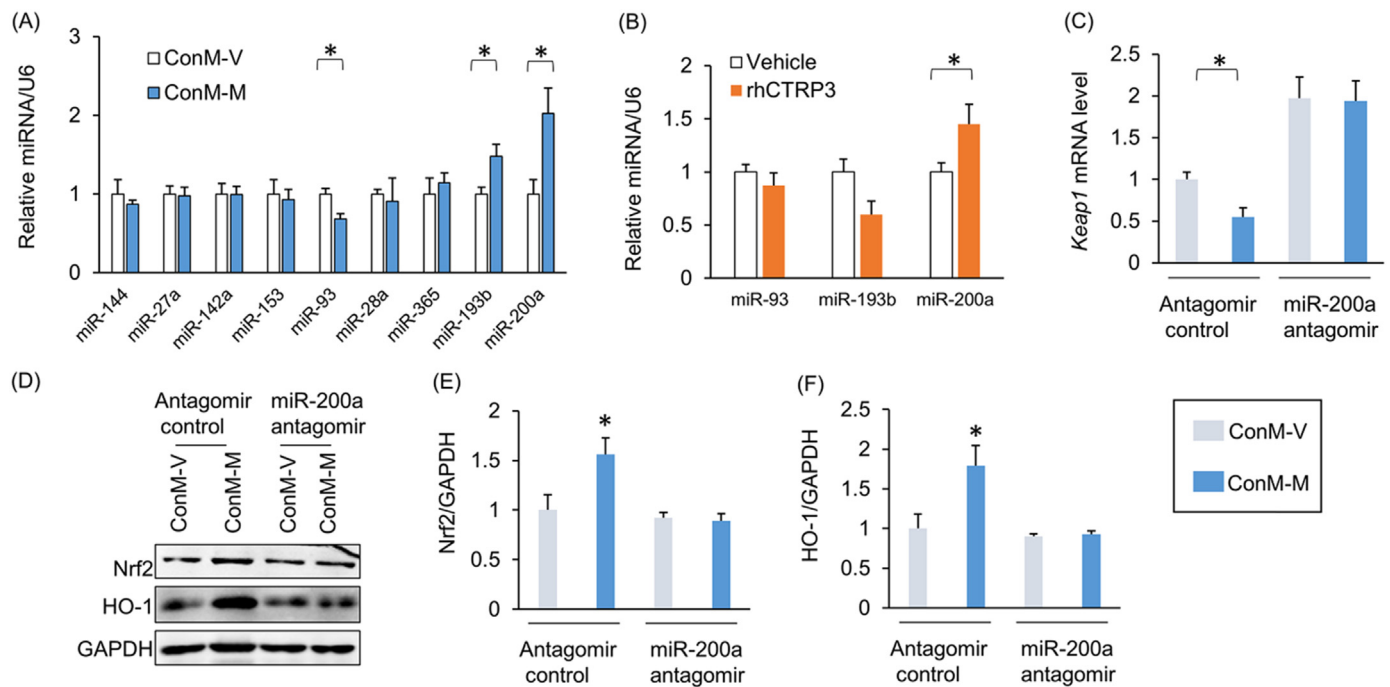


Fig. 7. miR-200a was closely associated with Nrf2 activation. (A) Nrf2-related miRNA levels. H9c2 cells were exposed to ConM-V or ConM-M for 24 h and then collected for further analysis. (B) miR-93a, miR-193b and miR-200a levels after rhCTRP3 treatment. (C) *Keap1* mRNA levels. (D–F) Nrf2 and HO-1 protein levels. rhCTRP3, recombinant human CTRP3. All data are expressed as the mean \pm SD of six independent experiments. Differences were compared by one-way ANOVA followed by Tukey's post hoc test. * $P < 0.05$.

circulating CTRP3 abolished the protective effects of melatonin, implying that direct crosstalk occurs between adipose tissue and the heart and that the crosstalk is guided by CTRP3 secretion.

Initial studies showed that CTRP3 was expressed predominantly by adipose tissue [9,26]. The data from a previous study indicated that CTRP3 is also expressed in the heart and that CTRP3 deficiency caused oxidative stress and cardiomyocyte apoptosis [10]. These findings imply that CTRP3 plays a key role in metabolic diseases. The finding that melatonin increases the CTRP3 expression in the adipocytes but not in the cardiomyocytes suggested that melatonin prevents obesity-related HFpEF independent of cardiomyocyte-derived CTRP3. This finding could be explained by the different abundance of CTRP3 in adipose tissue and heart. To date, the function of adipocyte-derived CTRP3 in the heart has not been intensively investigated. It has been reported that conditioned medium in which 3T3-L1 cells were cultured protected cardiomyocytes against hypoxia-induced cell death, an effect mediated by hypoxia inducing factor-1 α [39]. Here, we found that Nrf2, a regulator of genes encoding antioxidant stress proteins, mediated the action of adipocyte-derived CTRP3, which increased Nrf2 expression and downstream protein expression and promoted Nrf2 translocation from the cytoplasm to the nucleus in recipient cardiomyocytes, thus suppressing oxidative stress and cell death. CTRP3 deficiency in adipocytes or Nrf2 deficiency in cardiomyocytes abrogated the protective effects offered by melatonin-conditioned medium in cardiomyocytes, suggesting that Nrf2 is closely associated with the protective effects of melatonin. A study reported that overexpression of glutathione peroxidase could preserve diastolic function in diabetic heart [40], implying a close association between oxidative injury and impaired diastolic function. Inhibition of cell loss caused by HFD could improve diastolic function [41]. In our study, we found that melatonin could attenuate myocardial oxidative injury and cell loss in the obese mice, suggesting that reduction of cell loss might mediate melatonin-mediated protection in diastolic function.

miRNA, a class of small non-coding RNAs, regulates protein expression by base-pairing to the complementary sequences of target genes [42]. We detected the miRNAs that regulate Nrf2 expression and

found that miR-200a is induced by conditioned medium in which melatonin-treated adipocytes were cultured or by CTRP3. miR-200a activated Nrf2 by targeting *Keap1* mRNA [30]. Previous studies reported that miR-200a ameliorates diabetic nephropathy [28]. Consistent with the findings of these studies, the findings of this study showed that conditioned medium-induced reductions in *Keap1* expression and elevations in Nrf2 expression in cardiomyocytes were offset by miR-200a inhibition, which also blunted the protective effect of melatonin-conditioned medium on cell viability.

One limitation in our study that cannot be ignored is that we did not evaluate the side effects of melatonin. The side effects of melatonin included dizziness and drowsiness [43]. Melatonin could interact with diabetes medications [43]. Further study is still needed to evaluate the side effects of melatonin.

5. Conclusions

In conclusion, we found that melatonin ameliorated obesity-related HFpEF by promoting adipose tissue-derived CTRP3 secretion. Our study has provided basic evidence for the application of melatonin in the treatment of HFpEF.

Acknowledgements

This study was supported by the National Natural Science Foundation of China (Grant nos. 81600189 and 81600191), the Scientific and Technological Project of Henan Province (Grant nos. 172102310531 and 201403015), the Education Department of Henan Province (Grant no. 16A320029)

Declarations of interest

None.

Appendix A. Supplementary material

Supplementary data associated with this article can be found in the online version at doi:10.1016/j.redox.2018.07.007.

References

- C.W. Yancy, M. Jessup, B. Bozkurt, J. Butler, D.J. Casey, M.H. Drazner, G.C. Fonarow, S.A. Geraci, T. Horwich, J.L. Januzzi, M.R. Johnson, E.K. Kasper, W.C. Levy, F.A. Masoudi, P.E. McBride, J.J. McMurray, J.E. Mitchell, P.N. Peterson, B. Riegel, F. Sam, L.W. Stevenson, W.H. Tang, E.J. Tsai, B.L. Wilkoff, 2013 ACCF/AHA guideline for the management of heart failure: a report of the American College of Cardiology Foundation/American Heart Association Task force on practice guidelines, *J. Am. Coll. Cardiol.* 62 (2013) e147–e239.
- R.J. Mentz, J.P. Kelly, T.G. von Lueder, A.A. Voors, C.S. Lam, M.R. Cowie, K. Kjeldsen, E.A. Jankowska, D. Atar, J. Butler, M. Fuizat, F. Zannad, B. Pitt, C.M. O'Connor, Noncardiac comorbidities in heart failure with reduced versus preserved ejection fraction, *J. Am. Coll. Cardiol.* 64 (2014) 2281–2293.
- T.E. Owan, D.O. Hodge, R.M. Herges, S.J. Jacobsen, V.L. Roger, M.M. Redfield, Trends in prevalence and outcome of heart failure with preserved ejection fraction, *N. Engl. J. Med.* 355 (2006) 251–259.
- L.M. Sparks, H. Xie, R.A. Koza, R. Mynatt, M.W. Hulver, G.A. Bray, S.R. Smith, A high-fat diet coordinately downregulates genes required for mitochondrial oxidative phosphorylation in skeletal muscle, *Diabetes* 54 (2005) 1926–1933.
- S. Boudina, S. Sena, H. Theobald, X. Sheng, J.J. Wright, X.X. Hu, S. Aziz, J.I. Johnson, H. Bugger, V.G. Zaha, E.D. Abel, Mitochondrial energetics in the heart in obesity-related diabetes: direct evidence for increased uncoupled respiration and activation of uncoupling proteins, *Diabetes* 56 (2007) 2457–2466.
- A.T. Turer, J.A. Hill, J.K. Elmquist, P.E. Scherer, Adipose tissue biology and cardiomyopathy: translational implications, *Circ. Res.* 111 (2012) 1565–1577.
- V.B. Patel, J. Mori, B.A. McLean, R. Basu, S.K. Das, T. Ramprasath, N. Parajuli, J.M. Penninger, M.B. Grant, G.D. Lopaschuk, G.Y. Oudit, ACE2 deficiency worsens epicardial adipose tissue inflammation and cardiac dysfunction in response to diet-induced obesity, *Diabetes* 65 (2016) 85–95.
- A. Schaffler, J. Weigert, M. Neumeier, J. Scholmerich, C. Buechler, Regulation and function of collagenous repeat containing sequence of 26-kDa protein gene product "cartonectin", *Obesity* 15 (2007) 303–313.
- A. Schaffler, C. Buechler, CTRP family: linking immunity to metabolism, *Trends Endocrinol. Metab.* 23 (2012) 194–204.
- Z.G. Ma, Y.P. Yuan, S.C. Xu, W.Y. Wei, C.R. Xu, X. Zhang, Q.Q. Wu, H.H. Liao, J. Ni, Q.Z. Tang, CTRP3 attenuates cardiac dysfunction, inflammation, oxidative stress and cell death in diabetic cardiomyopathy in rats, *Diabetologia* 60 (2017) 1126–1137.
- R.J. Reiter, D.X. Tan, J. Cabrera, D. D'Arpa, Melatonin and tryptophan derivatives as free radical scavengers and antioxidants, *Adv. Exp. Med. Biol.* 467 (1999) 379–387.
- R.J. Reiter, D.X. Tan, C. Osuna, E. Gitto, Actions of melatonin in the reduction of oxidative stress. A review, *J. Biomed. Sci.* 7 (2000) 444–458.
- R.J. Reiter, D.X. Tan, M.J. Jou, A. Korkmaz, L.C. Manchester, S.D. Paredes, Biogenic amines in the reduction of oxidative stress: melatonin and its metabolites, *Neuro Endocrinol. Lett.* 29 (2008) 391–398.
- R.J. Reiter, D.X. Tan, Melatonin: a novel protective agent against oxidative injury of the ischemic/reperfused heart, *Cardiovasc. Res.* 58 (2003) 10–19.
- T. Wolden-Hanson, D.R. Mitton, R.L. McCants, S.M. Yellon, C.W. Wilkinson, A.M. Matsumoto, D.D. Rasmussen, Daily melatonin administration to middle-aged male rats suppresses body weight, intraabdominal adiposity, and plasma leptin and insulin independent of food intake and total body fat, *Endocrinology* 141 (2000) 487–497.
- A. Agil, M. Navarro-Alarcon, R. Ruiz, S. Abuhamadah, M.Y. El-Mir, G.F. Vazquez, Beneficial effects of melatonin on obesity and lipid profile in young Zucker diabetic fatty rats, *J. Pineal Res.* 50 (2011) 207–212.
- H. Kato, G. Tanaka, S. Masuda, J. Ogasawara, T. Sakurai, T. Kizaki, H. Ohno, T. Izawa, Melatonin promotes adipogenesis and mitochondrial biogenesis in 3T3-L1 preadipocytes, *J. Pineal Res.* 59 (2015) 267–275.
- Z. Liu, L. Gan, Y. Xu, D. Luo, Q. Ren, S. Wu, C. Sun, Melatonin alleviates inflammation-induced pyroptosis through inhibiting NF-kappaB/GSDMD signal in mice adipose tissue, *J. Pineal Res.* 63 (2017).
- Z.G. Ma, J. Dai, W.Y. Wei, W.B. Zhang, S.C. Xu, H.H. Liao, Z. Yang, Q.Z. Tang, Asiatic acid protects against cardiac hypertrophy through activating AMPKalpha signalling pathway, *Int. J. Biol. Sci.* 12 (2016) 861–871.
- Z.G. Ma, J. Dai, W.B. Zhang, Y. Yuan, H.H. Liao, N. Zhang, Z.Y. Bian, Q.Z. Tang, Protection against cardiac hypertrophy by geniposide involves the GLP-1 receptor/AMPKalpha signalling pathway, *Br. J. Pharmacol.* 173 (2016) 1502–1516.
- Z.G. Ma, Y.P. Yuan, X. Zhang, S.C. Xu, S.S. Wang, Q.Z. Tang, Piperine attenuates pathological cardiac fibrosis via PPAR-gamma/AKT pathways, *EBioMedicine* 18 (2017) 179–187.
- S.C. Xu, Z.G. Ma, W.Y. Wei, Y.P. Yuan, Q.Z. Tang, Bezafibrate attenuates pressure overload-induced cardiac hypertrophy and fibrosis, *PPAR Res.* 2017 (2017) 5789714.
- W.Y. Wei, Z.G. Ma, S.C. Xu, N. Zhang, Q.Z. Tang, Pioglitazone protected against cardiac hypertrophy via inhibiting AKT/GSK3beta and MAPK signaling pathways, *PPAR Res.* 2016 (2016) 9174190.
- K. Yamamoto, T. Masuyama, Y. Sakata, N. Nishikawa, T. Mano, J. Yoshida, T. Miwa, M. Sugawara, Y. Yamaguchi, T. Ookawara, K. Suzuki, M. Hori, Myocardial stiffness is determined by ventricular fibrosis, but not by compensatory or excessive hypertrophy in hypertensive heart, *Cardiovasc. Res.* 55 (2002) 76–82.
- W.J. Paulus, C. Tschöpe, A. Novel, Paradigm for Heart Failure With Preserved Ejection Fraction, *J. Am. Coll. Cardiol.* 62 (2013) 263–271.
- J.M. Peterson, Z. Wei, G.W. Wong, C1q/TNF-related protein-3 (CTRP3), a novel adipokine that regulates hepatic glucose output, *J. Biol. Chem.* 285 (2010) 39691–39701.
- D. Ayers, Baron, B., T. Hunter, miRNA influences in NRF2 pathway interactions within cancer models, *J. Nucleic Acids* 2015 (2015) 143636.
- H. Wu, L. Kong, Y. Tan, P.N. Epstein, J. Zeng, J. Gu, G. Liang, M. Kong, X. Chen, L. Miao, L. Cai, C66 ameliorates diabetic nephropathy in mice by both upregulating NRF2 function via increase in miR-200a and inhibiting miR-21, *Diabetologia* 59 (2016) 1558–1568.
- J.W. Kaspar, S.K. Niture, A.K. Jaiswal, Nrf2:INrf2 (Keap1) signaling in oxidative stress, *Free Radic. Biol. Med.* 47 (2009) 1304–1309.
- G. Eades, M. Yang, Y. Yao, Y. Zhang, Q. Zhou, miR-200a regulates Nrf2 activation by targeting Keap1 mRNA in breast cancer cells, *J. Biol. Chem.* 286 (2011) 40725–40733.
- D.X. Tan, L.C. Manchester, L. Fuentes-Broto, S.D. Paredes, R.J. Reiter, Significance and application of melatonin in the regulation of brown adipose tissue metabolism: relation to human obesity, *Obes. Rev.* 12 (2011) 167–188.
- B. Prunet-Marcassus, M. Desbazeille, A. Bros, K. Louche, P. Delagrang, P. Renard, L. Casteilla, L. Penicaud, Melatonin reduces body weight gain in Sprague Dawley rats with diet-induced obesity, *Endocrinology* 144 (2003) 5347–5352.
- R.J. Reiter, L.C. Manchester, L. Fuentes-Broto, D.X. Tan, Cardiac hypertrophy and remodelling: pathophysiological consequences and protective effects of melatonin, *J. Hypertens.* 28 (Suppl 1) (2010) S7–S12.
- A.S. Antonopoulos, M. Margaritis, S. Verheule, A. Recalde, F. Sanna, L. Herdman, C. Psarros, H. Nasrallah, P. Coutinho, I. Akoumianakis, A.C. Brewer, R. Sayeed, G. Krasopoulos, M. Petrou, A. Tarun, D. Tousoulis, A.M. Shah, B. Casadei, K.M. Channon, C. Antoniades, Mutual regulation of epicardial adipose tissue and myocardial redox state by PPAR-gamma/adiponectin signalling, *Circ. Res.* 118 (2016) 842–855.
- X. Fang, M.J. Stroud, K. Ouyang, L. Fang, J. Zhang, N.D. Dalton, Y. Gu, T. Wu, K.L. Peterson, H.D. Huang, J. Chen, N. Wang, Adipocyte-specific loss of PPARgamma attenuates cardiac hypertrophy, *JCI Insight* 1 (2016) e89908.
- S.R. Mahadik, S.S. Deo, S.D. Mehtalia, Association of adiposity, inflammation and atherosclerosis: the role of adipocytokines and CRP in Asian Indian subjects, *Metab. Syndr. Relat. Disord.* 6 (2008) 121–128.
- T. Hara, H. Fujiwara, T. Shoji, T. Mimura, H. Nakao, S. Fujimoto, Decreased plasma adiponectin levels in young obese males, *J. Atheroscler. Thromb.* 10 (2003) 234–238.
- K. Tanaka, R.M. Wilson, E.E. Essick, J.L. Duffen, P.E. Scherer, N. Ouchi, F. Sam, Effects of adiponectin on calcium-handling proteins in heart failure with preserved ejection fraction, *Circ. Heart Fail.* 7 (2014) 976–985.
- W. Yi, Y. Sun, Y. Yuan, W.B. Lau, Q. Zheng, X. Wang, Y. Wang, X. Shang, E. Gao, W.J. Koch, X.L. Ma, C1q/tumor necrosis factor-related protein-3, a newly identified adipokine, is a novel antiapoptotic, proangiogenic, and cardioprotective molecule in the ischemic mouse heart, *Circulation* 125 (2012) 3159–3169.
- S. Matsushima, S. Kinugawa, T. Ide, H. Matsusaka, N. Inoue, Y. Ohta, T. Yokota, K. Sunagawa, H. Tsutsui, Overexpression of glutathione peroxidase attenuates myocardial remodeling and preserves diastolic function in diabetic heart, *Am. J. Physiol. Heart Circ. Physiol.* 291 (2006) H2237–H2245.
- E. Ramirez, M. Klett-Mingo, S. Ares-Carrasco, B. Picatoste, A. Ferrarini, F.J. Ruperez, A. Caro-Vadillo, C. Barbas, J. Egido, J. Tunon, O. Lorenzo, Eplerenone attenuated cardiac steatosis, apoptosis and diastolic dysfunction in experimental type-II diabetes, *Cardiovasc Diabetol.* 12 (2013) 172.
- S. Ikeda, S.W. Kong, J. Lu, E. Bisping, H. Zhang, P.D. Allen, T.R. Golub, B. Pieske, W.T. Pu, Altered microRNA expression in human heart disease, *Physiol. Genom.* 31 (2007) 367–373.
- N. Buscemi, B. Vandermeer, N. Hooton, R. Pandya, L. Tjosvold, L. Hartling, S. Vohra, T.P. Klassen, G. Baker, Efficacy and safety of exogenous melatonin for secondary sleep disorders and sleep disorders accompanying sleep restriction: meta-analysis, *BMJ* 332 (2006) 385–393.